



OPEN Integrating bioinformatics and metabolomics to identify potential biomarkers of hypertensive nephropathy

Kezhen Yang^{1,6✉}, Pingna Zhang^{2,6}, Xiaofeng Ding^{3,6}, Gong Yu⁴, Jipeng Liu⁴, Yi Yang⁴, Jianqiao Fang⁵, Qingguo Liu⁴, Lu Zhang¹, Jianhua Li¹ & Fangchao Wu^{1✉}

Hypertensive nephropathy (HN), caused by long-term poorly controlled hypertension, is the second common cause of end-stage renal disease after diabetes mellitus, but the pathogenesis of HN is unclear. The purpose of this study was to identify the biological pathways involved in the progression of HN and bile acid (BA)-related biomarkers, and to analyze the role of bile acids in HN. Download gene microarray data from Gene Expression Omnibus. Differentially expressed genes (DEGs) associated with HN were identified, and then DEGs were subjected to Gene Ontology and Kyoto Encyclopedia of Genes and Genomes enrichment analysis. A protein–protein interaction (PPI) network was established using DEGs to identify BA-related hub genes in combination with bile acid identical targets. An animal model of early hypertensive nephropathy was established using SHR and the concentrations of 39 bile acids were measured quantitatively in the renal cortex to screen for significantly different concentrations and to analyze the correlation between bile acid concentrations and blood pressure. A total of 398 DEGs were screened. The results of enrichment analysis identified multiple biological pathways associated with hypertension, nephropathy and bile acids. Combining PPI network and bile acid-related targets, three BA-related hub genes (APOE, ALB, SERPINA1) were identified. Quantitative analysis of bile acids revealed significant differences in the concentrations of seven bile acids (DCA, CDCA, UDCA, UCA, CA, TDCA, TCDCA). The concentrations of these bile acids showed a positive correlation with blood pressure values in SHR, with CA, DCA and TDCA showing a stronger correlation and specificity with blood pressure in SHR. Three BA-related hub genes (APOE, ALB, SERPINA1) may be involved in the early stages of HN. The concentrations of multiple bile acids were significantly elevated in the early stages of HN, with CA, DCA and TDCA being more correlated and specific with blood pressure and having higher diagnostic value. These BA-related hub genes and BAs may be involved in disease progression in the early stages of HN.

Keywords Bioinformatic, Metabolomics, Hypertensive nephropathy, Bile acid, Bile acid metabolism

Hypertension is a multifactorial disease that exerts deleterious effects on cardiovascular and renal systems to end organ diseases with high morbidity and mortality¹. Hypertensive nephropathy (HN), as the second common causes of end-stage renal disease after diabetes, is mediated by poorly controlled hypertension for long term². At present, approximately 16% of patients suffering from hypertension also exhibit severe hypertensive nephropathy³. In addition, given that aging of the population and increased survival of cardiovascular diseases,

¹Department of Rehabilitation Medicine, Sir Run Run Shaw Hospital, Zhejiang University School of Medicine, 3 East Qingchun Road, Hangzhou 310016, Zhejiang, China. ²Department of Nephrology, The First Affiliated Hospital of Zhejiang Chinese Medical University (Zhejiang Provincial Hospital of Chinese Medicine), Hangzhou, China. ³Shanghai Skin Disease Hospital, School of Medicine, Tongji University, Shanghai, China. ⁴School of Acupuncture-Moxibustion and Tuina, Beijing University of Chinese Medicine, Beijing 102488, China. ⁵Key Laboratory of Acupuncture and Neurology of Zhejiang Province, The Third School of Clinical Medicine, Zhejiang Chinese Medical University, Hangzhou 310053, China. ⁶These authors contributed equally: Kezhen Yang, Pingna Zhang and Xiaofeng Ding. ✉email: 767299632@qq.com; 3414030@zju.edu.cn

and it is anticipated that the incidence of hypertensive nephropathy will increase in the coming years⁴. The pathophysiology of HN involves in multiple levels including vascular, glomerular, and tubulointerstitial levels⁵. Bioinformatics is a field of study that can be utilised to explore the molecular mechanisms associated with disease phenotypes. Previous studies have identified a variety of genes that may play significant roles in the progression of hypertensive nephropathy, including CYP3A4⁶, DUSP1⁷, POLR2I⁸, and some microRNAs⁹. Consequently, bioinformatics can contribute to a more comprehensive understanding of the underlying mechanisms of hypertensive nephropathy.

In a previous study, we found that abnormal Bile acids (BAs) metabolism may be involved in the pathogenesis of early renal injury in hypertension¹⁰. BAs function as signaling molecules via activation of BA receptors to regulate a wide range of metabolic processes, which involve in lipid and glucose homeostasis, energy expenditure, inflammation, and modulation of immune responses¹¹. The intimate connection between abnormal BA metabolism, its receptors such as FXR and the TGR5, and kidney diseases have been investigated^{12,13}. It has been shown that BAs as potential mediators in the gut-kidney axis involved in the pathophysiology of hypertension and chronic kidney disease (CKD)¹⁴. Furthermore, the several researches gradually found that BAs regulate blood pressure through modulating inflammatory response, vascular calcification and water homeostasis, and as potential novel targets in hypertension¹⁵. However, our understanding of the relationship between BAs and their biomarkers and the molecular mechanism of BAs involved in HN is still limited.

In order to further explore the potential link between BAs and HN, in this study, we analyzed the biological pathways associated with HN, constructed a protein–protein interaction (PPI) network, and identified hub genes associated with BA in combination with BA-related targets. Furthermore, we applied targeted metabolomics in spontaneously hypertensive rats (SHRs) to quantify the concentration of BAs in the renal cortex, and analyzed correlation with blood pressure in SHR, which introduces new insights into HN. The analysis process of this study is shown in Fig. 1.

Methods

Microarray data

The gene dataset used in the study was obtained from the National Center for Biotechnology Information publicly available Gene Expression Omnibus (GEO) database (<https://www.ncbi.nlm.nih.gov/geo/>). A series of matrix files of the dataset (GSE37460, GSE37455) were downloaded after normalization. Samples in the exploratory cohort and the validation Cohort were patients with a confirmed diagnosis of hypertensive nephropathy and healthy subjects, and kidney tissue was obtained for analysis at the time of kidney biopsy. GSE37460 was used as an exploration cohort, containing a total of 69 samples, and the extracted sites were glomeruli generated from renal biopsies. Five healthy controls and 15 patients with HN were selected for analysis, platform number GPL14663. GSE37455 was used as the validation cohort, containing a total of 41 samples, and the extracted sites were renal tubules generated from renal biopsies. Three healthy controls and 20 patients with HN were selected for analysis, platform number GPL14663.

Differentially expressed genes screening

After obtaining the raw data, the sample data were clustered using the “hclust function (method = “average”)” of the R software to observe the clustering between different groups and to eliminate obvious outliers. Differentially expressed genes (DEGs) between HN and healthy groups were identified using the Limma, a program package of the R software (v4.2.0, USA, 2024/1). The screening criteria were P value < 0.05 and $|\log(\text{fold change})| > 1.5$. A volcano diagram was used to demonstrate the identification process of DEGs.

Identified biological pathways of DEGs

All DEGs were imported into the Metascape database (<https://metascape.org/>) for Gene Ontology (GO) and Kyoto Encyclopedia of Genes and Genomes (KEGG) pathway analysis^{16–18}. The enrichment analysis was limited to the species “Homo sapiens” and the screening criteria for the analysis were min Overlap = 3, P value cut-off = 0.01, and min enrichment = 1.5. GO enrichment analysis included biological process (BP), cell composition (CC) and molecular function (MF). The results of the enrichment analysis were ranked according to the P value. Download all analysis results when the analysis is complete, the results of the analysis were visualized using the “ggplot2” program of the R software.

Construction of PPI network and identification of hub genes

All DEGs were imported into the STRING database (<https://cn.string-db.org/>) and used to construct protein–protein interaction (PPI) networks to characterize functional and physical interactions in the disease process of HN. The species restriction was “Homo sapiens” and the PPI information was extracted using an interaction score of 0.4. Visualization of the PPI interaction network was achieved with Cytoscape software (v3.9.1, USA, 2024/1) (<http://cytoscape.org/ver.3.9.1>)¹⁹. To explore hub genes, which are most closely related to HN, we used CytoHubba (<http://apps.cytoscape.org/apps/cytohubba>), a plug-in for Cytoscape, for hub gene identification. Four topological algorithms (Maximum neighborhood component (MCC), Degree, Maximum neighborhood component (MNC) and Closeness) were used to identify the top 10 scoring targets from the PPI network, and the results of the four methods were intersected to identify the hub genes.

Data validation

Based on the gene expression data of each sample, a box-and-line plot was used to show the expression of hub genes in different groups. In addition, Receiver operating characteristic (ROC) curves were used to predict the diagnostic value of the identified genes by calculating the area under the curve (AUC), sensitivity and

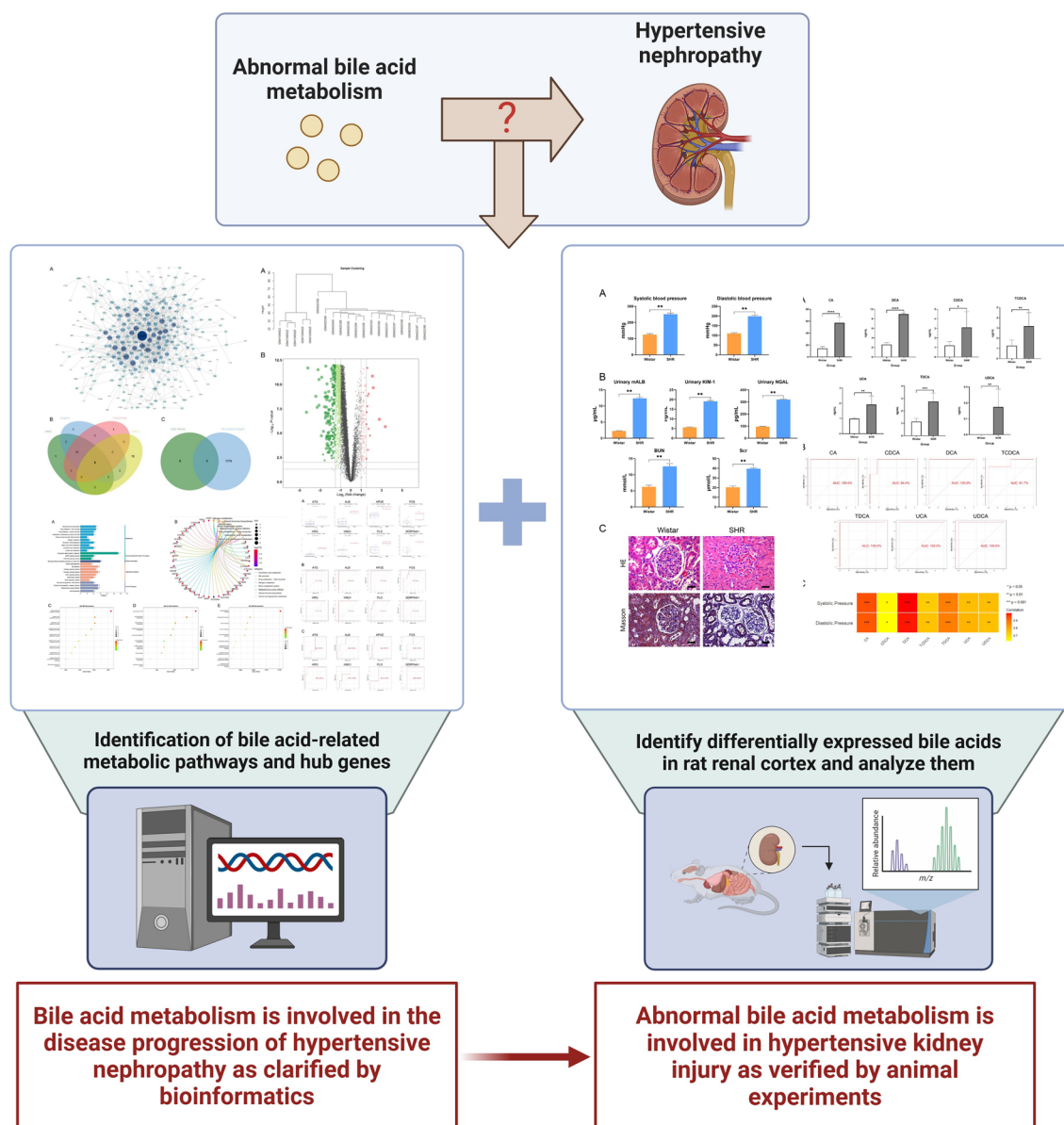


Fig. 1. Research flow chart.

1-specificity²⁰. The microarray dataset GSE37455 was used as a validation set to further verify the reliability of hub genes. After HN and healthy samples were selected, using the same processing methods as for the exploratory cohort, and the sample data were subjected to cluster analysis, and outlier sample data were excluded according to the clustering. Hub genes were placed in this dataset for validation, and genes with AUC > 0.7 were considered to have diagnostic value, and those with AUC > 0.8 were considered to have high diagnostic value. The AUC values of the exploration cohort and the validation cohort were compared to determine the diagnostic value of the hub genes.

Identification of BA-related hub genes

The keyword “Bile acid” was searched in the Genecards database (<https://www.genecards.org/>). All the pathways related to BA were identified, and all the targets in these pathways were obtained, merged and de-duplicated, and a total of 1173 targets were obtained (Supplementary Table S1). These targets were considered to be BA-related targets. Hub genes were used to intersect with BA-related targets to identify hub genes associated with BAs.

Animal models of hypertension

Six male Wistar rats (24 weeks old, 200 ± 10 g) and six male spontaneously hypertensive rats (24 weeks old, 200 ± 10 g) were provided by Beijing Viton Lihua Experimental Animal Technology Co. Wistar rats were used as the control group (Wistar group) and SHR rats were used as the model group (SHR group) and were housed in the laboratory of Beijing University of Chinese Medicine (SPF level). The Animal Care and Utilization Committee

of Beijing University of Traditional Chinese Medicine approved this study (BUCM-4-2021-041001-2093). This research report was conducted in accordance with the relevant guidelines and regulations and also all methods are reported in accordance with ARRIVE guidelines²¹. The model was selected from 24-week-old SHR rats, a week-old rat that has begun to show signs of kidney injury. The rats were housed in the same environment and suitable for survival and were acclimatized and fed for one week before performing the operation. Tail artery blood pressure was measured in all rats using a noninvasive blood pressure monitor (Beijing Zhongshi Dichuang Technology Development Co., Ltd.). The mean of three consecutive measurements was used as the blood pressure value for this measurement to observe the success of the hypertensive rat model.

Biochemical measurements

The day before the rats were executed, all rats in each group were placed in metabolic cages to collect urine for kidney injury indicators (mALB, NGAL, KIM-1). All renal injury indicators were tested according to the manufacturer's instructions (Shanghai Enzyme-linked Biotechnology Co., Ltd. Shanghai, China). The rats were fasted for 12 h and injected intraperitoneally with 35 mg/kg pentobarbital sodium followed by blood collection from the abdominal aorta. Serum was collected for the detection of blood creatinine and urea nitrogen. All biochemical parameters were assayed according to the manufacturer's instructions (Nanjing Jiancheng Bioengineering Institute, Nanjing, China).

Pathological examination of renal tissue

All rats were executed, and the kidney tissues of all rats was extracted for subsequent analysis. Kidney tissues of different groups were sequentially fixed in 4% paraformaldehyde, dehydrated in ethanol and embedded in paraffin. Paraffin sections (3 µm) were subjected to H&E staining and Masson staining. All samples were observed by a light microscope (400× magnification).

Quantitative analysis of BAs

Preparation of BAs standard solution

Weigh the appropriate amount of 39 BAs standards, measure the appropriate amount of each master batch to make mixed standards, dilute them one by one with methanol (Thermo) to the appropriate concentration to make working standard solutions, and store both the master batch and working standard solutions at − 20 °C. The information of various BAs concentration gradients is shown in supplementary Table S2.

Liquid chromatograph-mass spectrometer analysis

Chromatographic separation of BAs was performed using a linear gradient elution mode on an ACQUITY UPLC[®] BEH C18 column (2.1 × 100 mm, 1.7 µm, Waters Corporation, USA). Mobile phase composition: (A) 0.01% formic acid in water (TCI), (B) acetonitrile (Thermo). Injection volume: 5 µL, column temperature: 40 °C. The BAs eluted from the column were ionized using electrospray ionization (ESI) source in negative ionization mode. Mass spectrometry parameters: ion source temperature of 500 °C, ion source voltage of − 4500 V. The ion pairs used for quantitative analysis are shown in supplementary Table S3.

Standard curve of BAs

The standard solutions of 39 BAs were detected by liquid chromatograph-mass spectrometer (LC-MS), and the standard curves of each BA concentration were plotted with the concentration gradient information as the horizontal coordinate and the peak area as the vertical coordinate. The obtained linear regression equations for various BAs are shown in Supplementary Table S4, with the correlation coefficients $r > 0.99$. The standard solutions of different concentrations of BAs were injected six times consecutively and the intra-day precision was calculated. The standard solutions of different concentrations of BAs were measured on different dates, and the inter-day precision was calculated. The intra-day precision of all BAs standard solutions ranged from 1.52 to 10.14%, and the inter-day precision ranged from 2.18 to 23.44%, indicating that the precision of the instrument was good. The results are shown in Supplementary Table S5.

Extraction and analysis of BAs

Precisely weigh 50 mg of each rat kidney cortex sample in a 2 mL eppendorf tube, add 1000 µL of methanol (Thermo) (− 20 °C), vortex shake for 60 s, then grind the tissue and repeat the above operation at least two times. The tissues were sonicated for 30 min at room temperature, followed by centrifugation at 4 °C for 10 min at 12,000 rpm. 200 µL of supernatant was mixed with 400 µL of aqueous solution and vortexed for 30 s. 300 µL of the supernatant was filtered through a 0.22 µm membrane (Jin Teng), and the filtrate was added to the assay bottle. The BAs in all samples were quantified according to the established sample pre-treatment and instrumental analysis methods. ROC analysis was performed in combination with the concentration of BAs, and AUC values were used to indicate the diagnostic value of BAs.

Statistical analysis

SPSS 20.0 (v20.0, USA, 2024/1) statistical software was used for statistical analysis of the data. Data were expressed as ($\bar{X} \pm S$). Student's t-test was used to analyze the differences between groups, and differences were expressed as P values. $P < 0.05$ was considered statistically different, and $P < 0.01$ was considered significantly different.

Result

Identification of DEGs in HN

By analyzing the microarray dataset from the GEO database, we screened the DEGs in the course of HN onset. The raw data from the dataset GSE37460 were processed with normalization criteria, and then the selected sample data were clustered and analyzed, and one outlier sample was excluded (GSM920389) (Fig. 2A). 398 DEGs (15 up-regulated and 383 down-regulated) were identified, and their volcano plots are shown in Fig. 2B.

Function enrichment analyses of the DEGs

GO and KEGG analysis was performed using Metascape to determine the biological significance of DEGs in HN^{22,23}. The KEGG pathway enrichment resulted in a total of 52 pathways, and we collected the 25 pathways with the smallest *P* values and presented them using bar and circle plots (Fig. 3A,B). The pathways involved include neuroactive ligand-receptor interaction, steroid hormone biosynthesis, bile secretion, AMPK signaling pathway, TGF-beta signaling pathway and renin-angiotensin system, among others. In the GO analysis, we show the 10

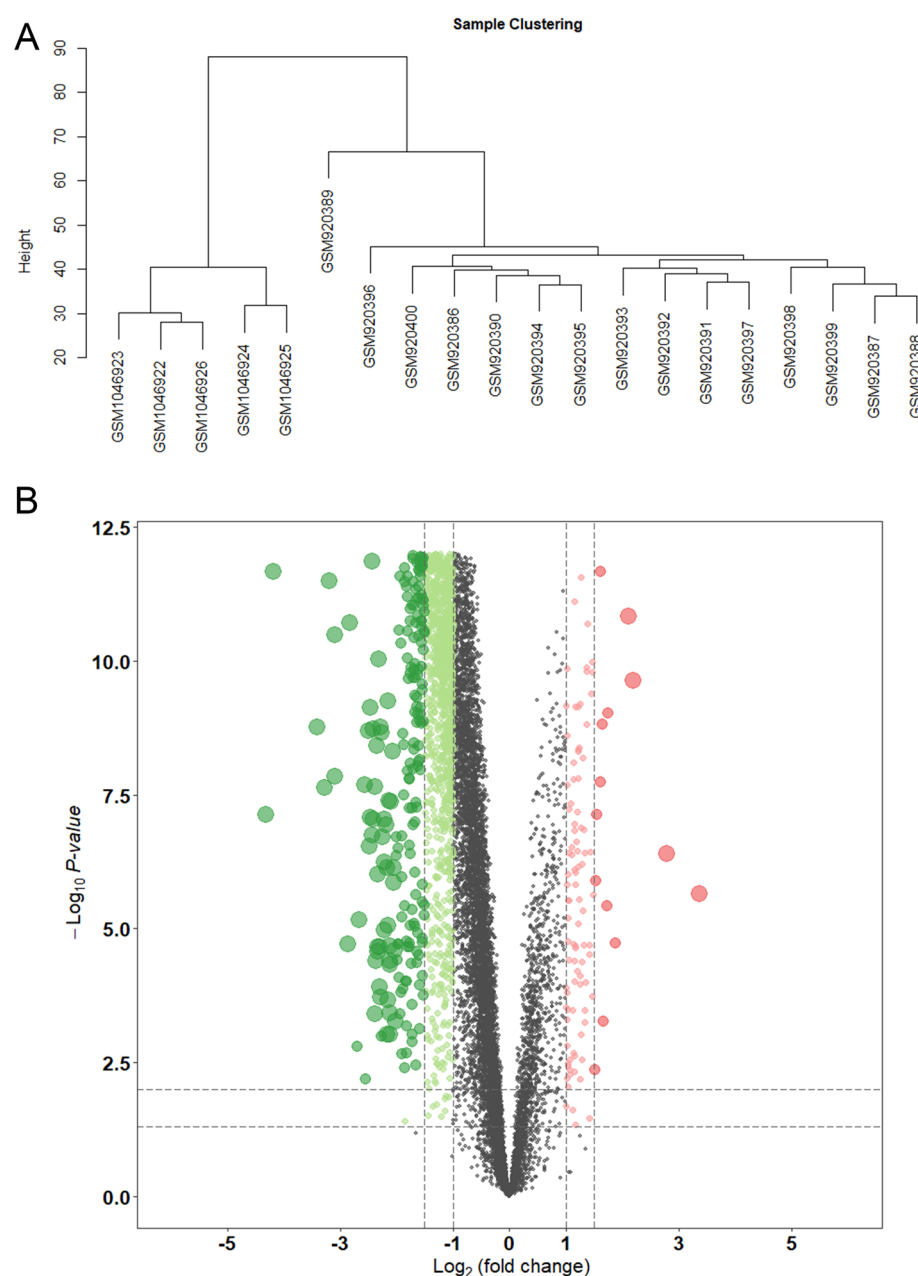


Fig. 2. Dataset characteristics and volcano plots of DEGs. **(A)** Sample analysis dendrogram to observe the presence of significant outlier samples. **(B)** Volcano diagram of DEGs. The green dots are downward DEGs, and the red dots are upward DEGs. The dashed lines on the x-axis correspond to $|\log(\text{fold change})| = 1$ and 1.5. The dashed lines on the Y-axis correspond to $P = 0.05$ and 0.01. DEGs,

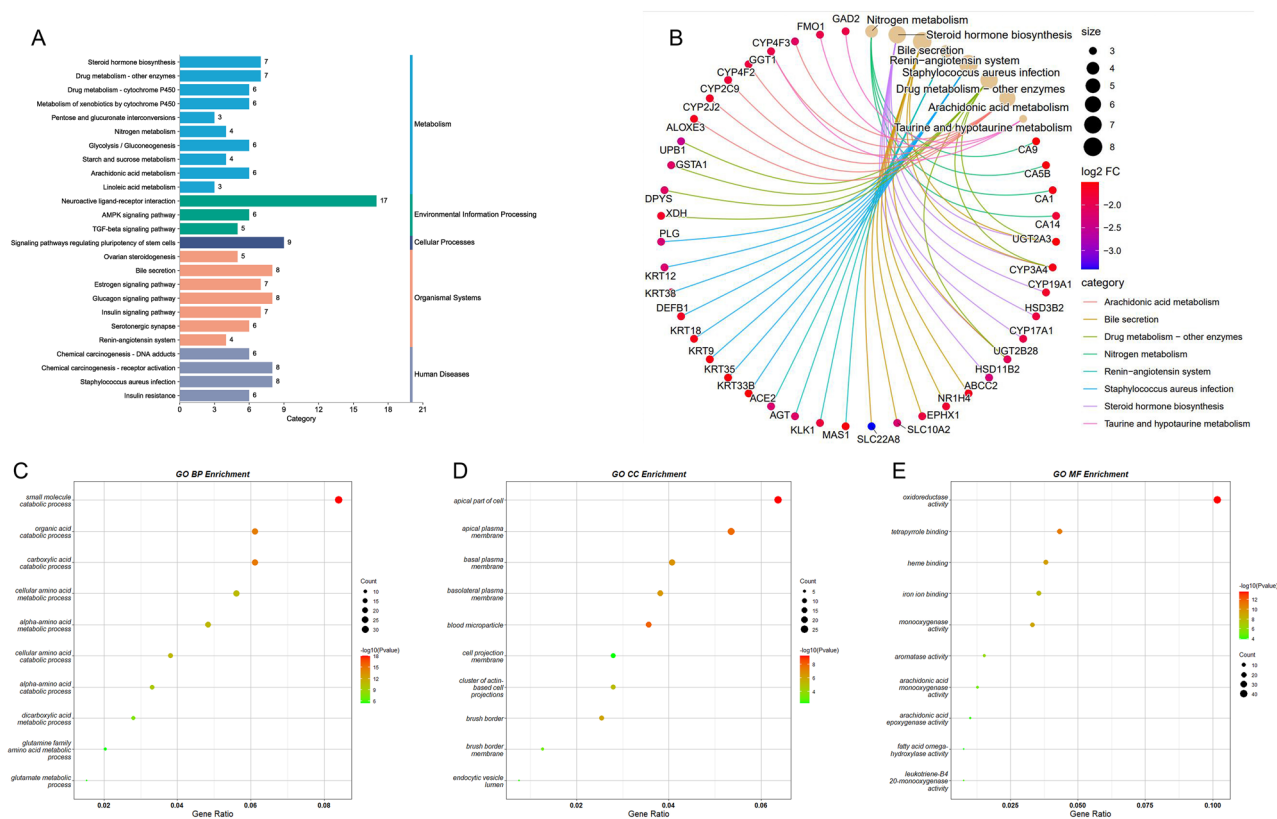


Fig. 3. Biological pathway enrichment analysis. **(A)** KEGG enrichment analysis bar graph (<http://www.KEGG.jp/KEGG/kegg1.html>). Different colors indicate different KEGG classifications. The horizontal axis indicates the number of genes annotated to the pathway. The vertical axis indicates the pathway name. **(B)** KEGG enrichment analysis circle diagram. The dots represent targets and pathways. The color of the dots corresponds to the log FC. **(C–E)** GO enrichment analysis. GO analysis includes BP, CC and MF. The size of the dot corresponds to the number of genes annotated to the term. The color of the dot corresponds to the P value of the term. FC, fold change. GO, gene ontology. KEGG, Kyoto encyclopedia of genes and genomes. BP, biological process. CC, cell composition. MF, molecular function.

terms with the smallest P -values in each category of BP, CC, and MF (Fig. 3C–E). In the GO BP category, a total of 593 terms were enriched, and most of the DEGs are mainly involved in the metabolic processes of multiple amino acids, as well as small molecule catabolic process, organic acid catabolic process and dicarboxylic acid metabolic process, etc. In the GO CC category, a total of 54 terms were enriched, and most of the DEGs were enriched in apical part of cell, apical plasma membrane. In the GO MF category, a total of 130 terms were enriched, and most of the DEGs were enriched in the areas of oxidoreductase activity, heme binding and tetrapyrrole binding.

Construction of PPI network and identification of BA-related hub genes

The PPI network built using DEGs includes a total of 313 nodes and 978 edges (Fig. 4A). In the protein network diagram, each nodes represents a protein, and edges represent the association between two neighboring proteins. Topology scores were calculated using four algorithms of CytoHubba (MCC, MNC, Degree and Closeness), and the 20 proteins with the highest scores were taken as intersections, and the overlaps were considered as hub genes of HN: HRG, AGT, APOE, ALB, FOS, KNG1, PLG, SERPINA1 (Fig. 4B). The intersection of hub genes and BA-related targets was taken, and the overlapping parts were considered as hub genes associated with BAs during HN, and a total of three genes were found: APOE, ALB, SERPINA1 (Fig. 4C).

Diagnostic value of BA-related hub genes in the exploration cohort and the validation cohort

In exploration cohort, box plot was used to demonstrate the expression of BA-related hub genes in different groups (Fig. 5A). In the ROC curve analysis, the AUC values of the three BA-related hub genes were used to assess the sensitivity and specificity to HN. The results showed that their AUC values were all equal to 1, indicating that these genes have a high diagnostic value for HN (Fig. 5B). We repeated the same analysis in the validation cohort, and the results showed that their AUC values were >0.8 (Fig. 5C). This indicates that the three BA-related hub genes have a high diagnostic value for HN.

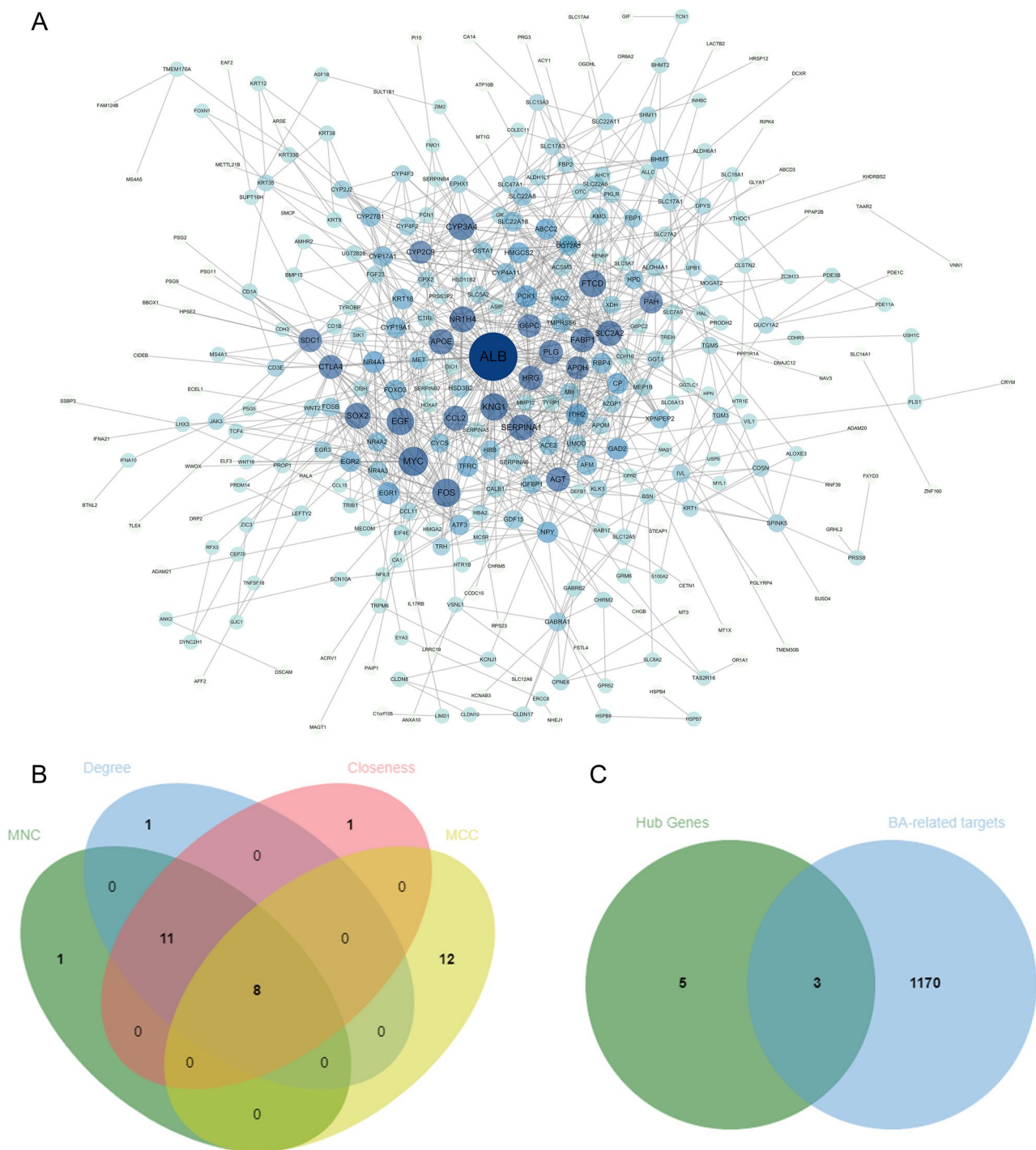


Fig. 4. Construction of PPI network and identification of hub genes. **(A)** PPI network diagram. Each point represents a gene. The higher the degree value, the darker the color of the dot and the larger the font size. **(B)** Venn diagram identifying the hub genes. **(C)** Venn diagram to identify BA-related hub genes. BA, bile acid. PPI, protein-protein interaction.

Blood pressure and kidney injury indicator tests

The measurements of systolic and diastolic blood pressure in the two groups of rats are shown in Fig. 6A. All measurements of systolic and diastolic blood pressure were significantly different between the two groups ($P < 0.01$), and the blood pressure in the SHR group was significantly higher than that in the Wistar group.

The results of renal function indexes in rats are shown in Fig. 6B. The levels of mALB, KIM-1, and NGAL in the urine of the SHR group were significantly higher than those of the Wistar group ($P < 0.01$); The levels of BUN and Scr in the serum of SHR were significantly higher than those of the Wistar group ($P < 0.01$). The staining results of rat kidney tissue structure are shown in Fig. 6C. HE stains showed that many inflammatory cells were

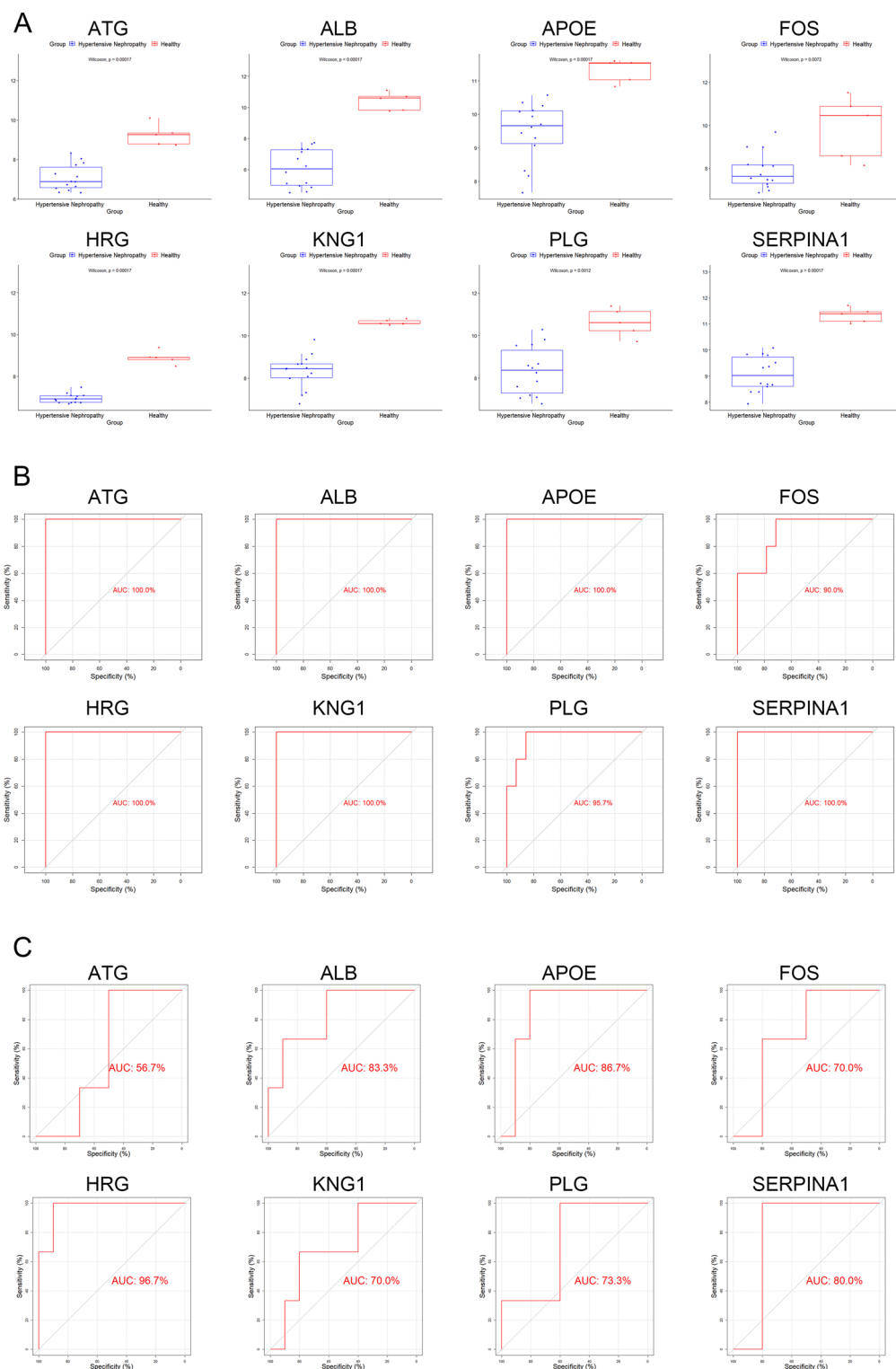


Fig. 5. Analysis of hub genes. **(A)** Hub genes expression box line plot. Different colors indicate different groups. **(B)** ROC analysis in the explore cohort. AUC indicates the area under the curve. **(C)** ROC analysis in the validate cohort. AUC, area under the curve. ROC, receiver operating characteristic.

infiltrated in some tissues of the kidneys in the SHR group. The brush border of renal tubules was detached, and the structure of some renal tubules was obviously abnormal, with unclear cell outlines; individual cells were necrotic and deformed, and cell nuclei were fragmented. Masson's staining showed increased collagen deposition

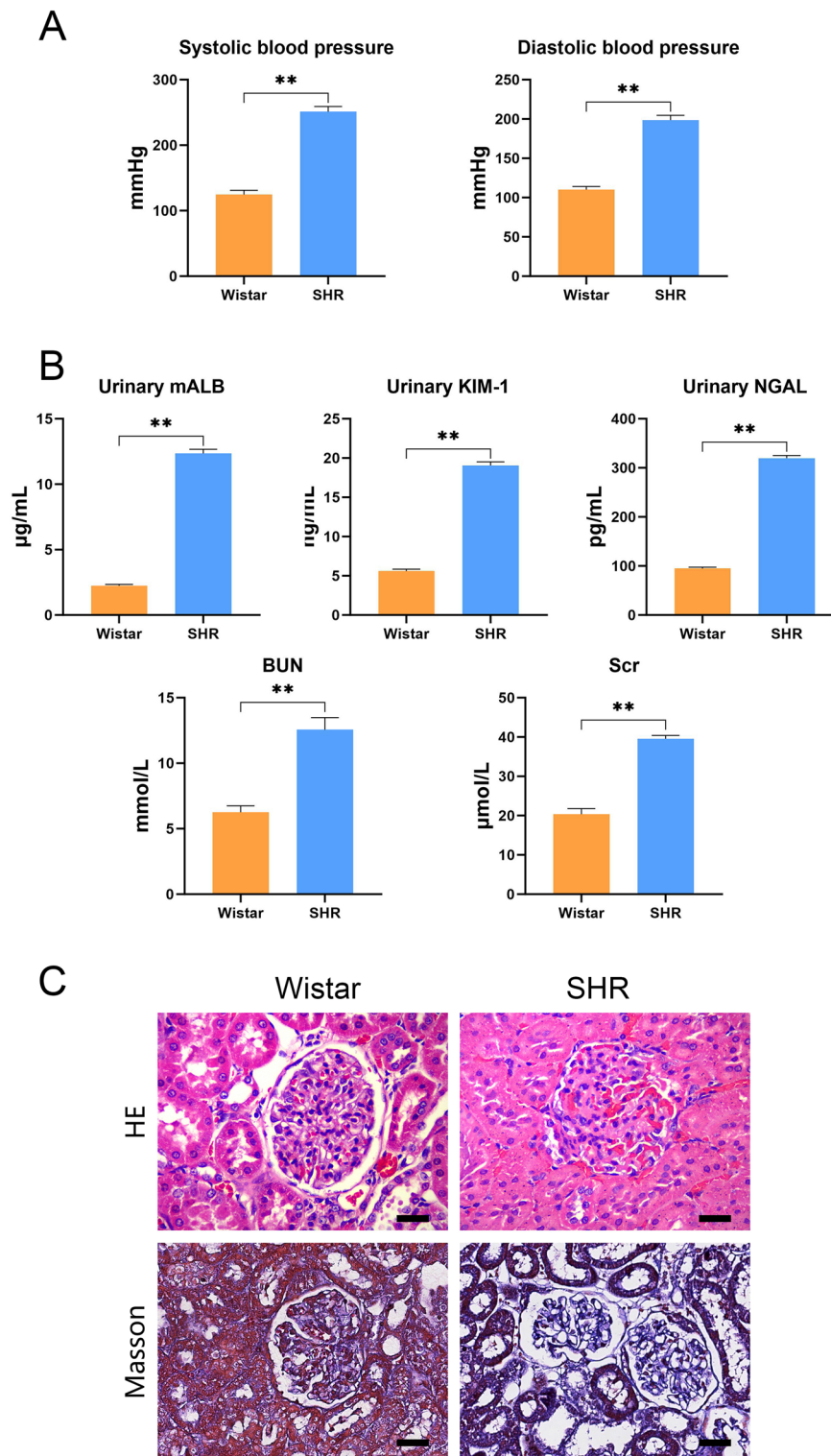


Fig. 6. Detection of blood pressure and kidney injury indexes in rats. (A) Analysis of blood pressure values in rats. (B) Results of renal function indexes in rats. (C) Structural HE and Masson staining of rat kidney ($\times 400$). ** $P < 0.01$. Bar = 100 μm . Bun, blood urea nitrogen. Scr, serum creatinine.

in the renal tissues of the SHR group. The above results indicated that the SHR group had elevated blood pressure and impaired renal function, and the animal model of hypertensive kidney injury was successfully established.

BAs measurement results

In the previous study, abnormal bile acid metabolism was found to be possibly involved in the progression of kidney injury in SHR by metabolomics^{10,24,25}. On this basis, to further clarify whether bile acid metabolism is involved in the development of hypertensive kidney injury in humans, first, the hub genes related to hypertensive nephropathy were identified by bioinformatics methods, and the information of targets related to the bile acid metabolism pathway was searched, and the hub genes related to bile acids in HN were found, and it can be clarified that bile acid metabolism is indeed involved in the disease progression of HN. To further clarify which type of bile acid is involved, bile acid-targeted metabolomics was performed on rat kidneys to detect the specific levels of multiple bile acids.

Thirty-nine BAs were detected in the renal cortex of rats in both groups using LC–MS analysis, and the concentration of each BA was measured. The concentration of some BAs were because their levels were below the detection limit and therefore not detected. The names and concentrations of all BAs are shown in Table 1. The BAs with significant differences between the SHR group and the Wistar group were: DCA, CDCA, UDCA, UCA, CA, TDCA, and TCDCA, as shown in Fig. 7A. Then, we analyzed the diagnostic value of these differential BAs using ROC curves, and the results showed that their AUC values were > 0.9, indicating that these differential BAs had a high diagnostic value (Fig. 7B).

Correlation between blood pressure and BAs

Next, we calculated Spearman correlations between blood pressure values and differential BAs in rats, and then visualized them using the "ggplot2" program package. It was found that there was a significant positive correlation between BAs concentrations and blood pressure values in rats (Fig. 7C). Among the BAs with stronger correlation and more significant differences were CA, DCA and TDCA. This suggests that these three BAs play a more important regulatory role in the pathogenesis of HN by regulating BAs.

Discussion

In this study, we identified hub genes that are closely associated with BAs in the pathogenesis of HN. Targeted metabolomic analysis of BAs in the renal cortex of SHR revealed significant changes in the concentrations of multiple BAs in the early stages of HN, and these BAs showed significant correlation and specificity with blood pressure values in SHR. These BA-related hub genes with BAs may become biomarkers and molecular targets closely related to HN.

HN is second only to diabetes as the leading cause of progressive chronic kidney disease. Hypertension affects every part of the kidney, including the blood vessels, glomeruli and tubules²⁶. Over time, it causes renal vascular sclerosis and hyalinosis, resulting in glomerular injury⁵, and afferent arteriolar stenosis in hypertensive patients leads to glomerular ischemia, making the glomeruli smaller and gradually reducing the filtration rate²⁷. At the same time, hypertension induces the transition of renal tubular epithelial cells to the mesenchyme and tubular interstitial fibrosis⁵, which can lead to extensive lesions in epithelial tubular cells²⁶. In animal experiments, at least one animal model of polygenic hypertension, the spontaneously hypertensive rat, supports the independence of the risk of hypertensive renal damage²⁸. In past studies, it was found^{10,24} that abnormal BA metabolism in the kidney of SHR rats may be an independent risk factor for the development of hypertension, and multiple BAs were found to be strongly associated with the development of hypertension.

By enrichment analysis of DEGs, we have identified biological pathways associated with the pathogenesis of HN. In BP, the enrichment results were associated with the metabolism of a variety of amino acids. Amino acids can form couples with bile acids and participate in the metabolic process of BAs²⁹. The results of CC suggest that these cellular components may be involved in the progression of HN, for example: the brush border membrane is differentially characterized in rats with different renal diseases³⁰. Changes in some genes of the basolateral plasma membrane of glandular alveolar cells were associated with hypertension-induced changes in sympathetic activity³¹. The results of MF found that oxidoreductase activity was most closely related to HN. Enrichment analysis of the KEGG pathway revealed that abnormal bile secretion and metabolism may be involved in the disease progression of HN, which is similar to the results of previous studies^{10,24}. In addition, some signaling pathways were found to be involved in HN. Autophagy can be enhanced by activating the AMPK signaling pathway to prevent Ang II-induced endothelial progenitor cell damage, which contributes to vascular endothelial repair in hypertensive patients³². The use of AMPK agonists also normalizes endothelium-dependent vasodilation and reduces blood pressure in rats³³. It has been found that by inhibiting the TGF- β signaling pathway, it can play an important regulatory role in Ang II-induced HN³⁴. Also, by regulating the TGF- β signaling pathway can alleviate renal injury in SHR and reduce tubulointerstitial fibrosis³⁵. RAS is mainly related to the regulation of blood pressure³⁶, and renal injury in a rat model of renal vascular hypertension can be attenuated by regulating RAS³⁷. The results of the enrichment analysis identified multiple biological pathways related to the pathogenesis of HN, among which Bile secretion is closely related to the direction of our study.

Next, we established a PPI network and combined it with BA-related genes to identify three BA-related hub genes in HN: APOE, ALB, and SERPINA1. APOE is a major component of plasma lipoproteins and has many important biological roles. There is increasing evidence that abnormalities in lipids may contribute to the development and progression of kidney disease^{38–42}. APOE has been found to be associated with the pathogenesis and progression of various renal diseases and may also influence the incidence of cardiovascular disease⁴³. The aortae of mice deficient in APOE spontaneously develop hyperlipidemia and atherosclerosis⁴⁴, and persistent hyperlipidemia leads to upregulation of oxidative and inflammatory factors in the kidney, ultimately causing kidney injury⁴⁵. Also, in a meta-analysis, an association was found between polymorphisms in APOE and hypertension, and genotypes of different alleles may have opposite effects on hypertension^{46,47}. ALB is the most abundant protein in human blood, it is widely accepted that albuminuria is a predictor of renal injury and kidney

Bile acid	Abbreviations	Wistar	SHR
Allolithocholic acid	alloLCA	0	0
Lithocholic acid	LCA	0	0
Isolithocholic acid	isoLCA	0	0
23-Nordeoxycholic acid	NorDCA	0	0.1 ± 0.25
6-ketolithocholic acid acetate	6-ketoLCA	0	0
12-ketolithocholic acid	12-ketoLCA	0	0.26 ± 0.29
7-ketolithocholic acid	7-ketoLCA	0	0
3β-Ursodeoxycholic acid	beta-UDCA	0	0
Deoxycholic acid	DCA	2.59 ± 0.41	8.97 ± 0.18***
Chenodeoxycholic acid	CDCA	1.2 ± 0.43	3.09 ± 1.67*
Ursodeoxycholic acid	UDCA	0	0.17 ± 0.11*
Hyodeoxycholic acid	HDCA	0.32 ± 0.49	3.07 ± 4.29
Norcholeic acid	NorCA	0.01 ± 0.02	0.02 ± 0.04
Dehydrocholic acid	DHCA	0	0.04 ± 0.07
7,12-diketolithocholic acid	7,12-diketoLCA	0	0
6,7-diketolithocholic acid	6,7-diketoLCA	0	0
α-Muricholic acid	alpha-MCA	1.39 ± 1.03	4.06 ± 2.57
Ursocholic acid	UCA	0.98 ± 0.06	1.92 ± 0.56**
β-Muricholic acid	beta-MCA	5.23 ± 1.72	31.88 ± 28.11
Cholic acid	CA	14.1 ± 3.34	57.02 ± 10.18***
Allocholeic acid	ACA	0	0
3β-Cholic acid	beta-CA	1.7 ± 0.42	1.85 ± 0.8
Glycolithocholic acid sodium salt	GLCA	0.15 ± 0.02	0.14 ± 0.01
Glycohyodeoxycholic acid	GHDCA	0.03 ± 0.04	0.02 ± 0.04
Glychenodeoxycholic acid sodium salt	GCDCA	0.22 ± 0.02	0.24 ± 0.03
Glycoursodeoxycholic acid	GUDCA	0.06 ± 0.05	0.08 ± 0.04
Glycodeoxycholic acid sodium salt	GDCA	0.2 ± 0.06	0.25 ± 0.05
Lithocholic acid 3-sulfate sodium salt	LCA-3S	0	0
Sodium glycocholate hydrate	GCA	2.1 ± 1.12	2.24 ± 0.57
Taurolithocholic acid sodium salt	TLCA	0.04 ± 0.04	0.03 ± 0.04
Taurohyodeoxycholic acid sodium salt + tauroursodeoxycholic acid sodium salt	THDCA + TUDCA	0.58 ± 0.9	0.28 ± 0.68
Taurodeoxycholic acid sodium salt	TDCA	1.14 ± 0.26	2.76 ± 0.65***
Taurochenodeoxycholic acid	TCDCa	1.26 ± 0.57	3.18 ± 1.33**
Taurocholic acid sodium salt	TCA	45.25 ± 30.94	68.29 ± 16.12
Tauro-α-muricholic acid sodium salt	T-alpha-MCA	13.3 ± 8.03	15.97 ± 3.91
Taurohyocholic acid sodium salt	THCA	0	0
Tauro-β-muricholic acid sodium salt	T-beta-MCA	13.13 ± 8.26	15.87 ± 4.19
Chenodeoxycholic acid glucuronide	CDCA-G	0.08 ± 0.09	0.09 ± 0.15

Table 1. Quantitative analysis of bile acid concentration. * $P < 0.05$, ** $P < 0.01$, *** $P < 0.001$, vs Wistar group.

disease⁴⁸. Clinically, albuminuria is also considered to be a marker of extensive vascular injury in hypertensive populations and is one of the clinical parameters associated with adverse outcomes⁴⁹. In one study⁵⁰, ALB was a SHR-specific gene involved in renal injury and also a candidate gene for causing SHR hypertension by a specific mechanism that may be related to angiotensinogen. The expression trend of ALB in the present study was not completely consistent with previous studies, probably due to the different sites of sampling, and the exact reason for this needs to be further investigated. SERPINA1 can encode an acute-phase protein that is synthesized in the liver. This protein has a wide range of biological roles, including anti-inflammatory and immunomodulatory, as well as interactions with serum lipoproteins^{51–54}. It has been shown that urinary levels of SERPINA1 are elevated in patients with primary and secondary hypertension⁵⁵, and urinary SERPINA1 has also been found to be significantly associated with systolic blood pressure and proteinuria⁵⁶. However, in another study it was found that reduced expression of A1AT encoded by SERPINA1 leads to an increased cardiovascular risk profile and potentially elevated cardiovascular disease risk⁵⁷. In a study of nephrotic syndrome, SERPINA1 was significantly elevated in the urine of patients with microscopic lesion disease, focal segmental glomerulosclerosis, and membranous nephropathy⁵⁸. These BA-related hub genes are not only associated with the pathogenesis of hypertension and nephropathy, but also can play a role in the regulation of BAs^{59,60}. They may be key to the progression of HN disease.

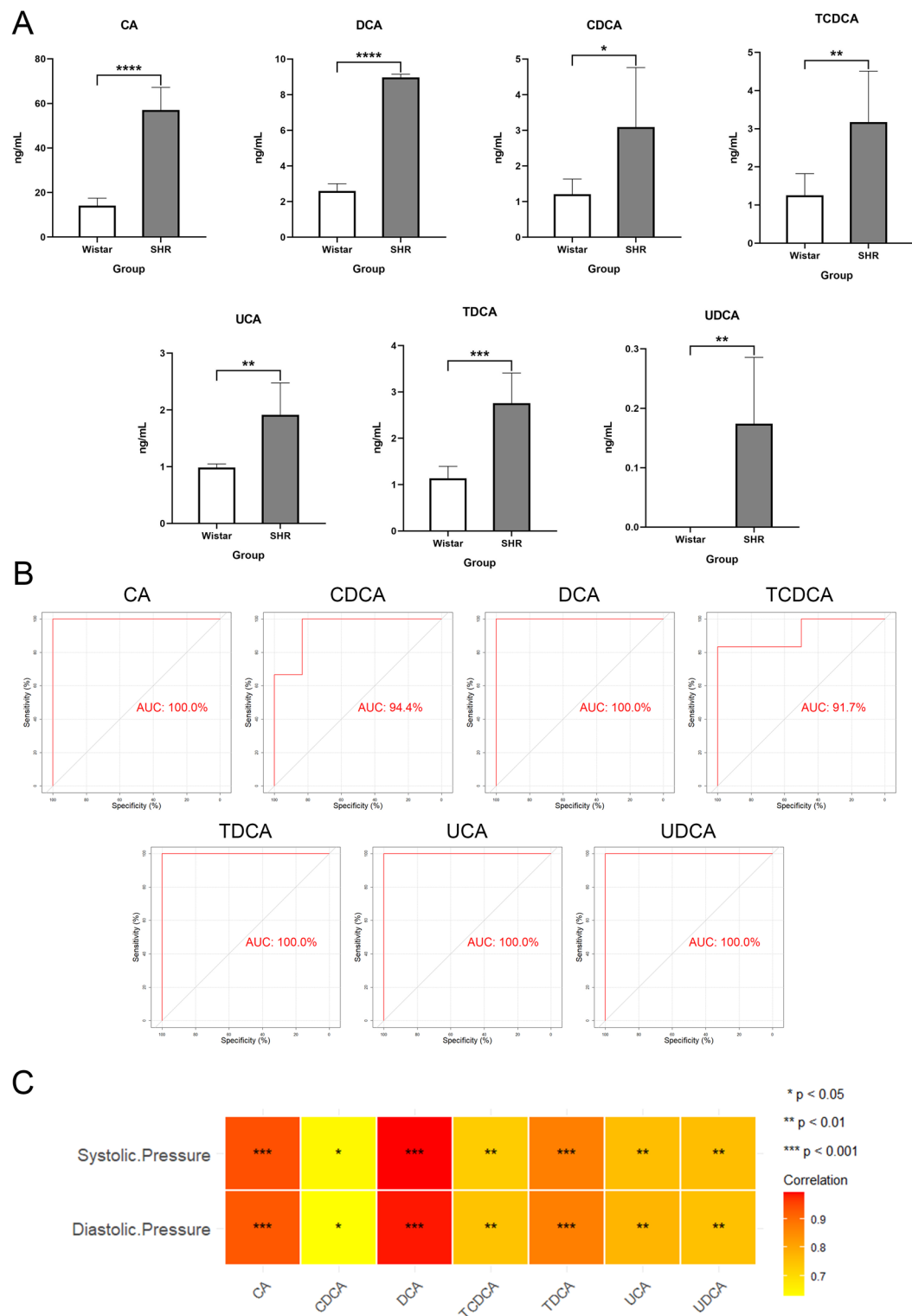


Fig. 7. Analysis of BAs. **(A)** Bar graphs of Bas content in different groups. **(B)** ROC analysis of BAs. **(C)** Correlation analysis between BAs and systolic blood pressure in rats. BA, bile acid. * $P < 0.05$, ** $P < 0.01$, *** $P < 0.001$, **** $P < 0.0001$.

SHR is usually considered a typical animal model of hypertension combined with renal injury, and some studies have found that renal injury further deepens with the age of SHR⁶¹. When SHR reaches 12 weeks of age, changes in indicators associated with renal injury begin to appear, but they have not yet shown significant

differences⁶². Until 30 weeks of age, hypertensive kidney injury is not yet morphologically evident^{63,64}. By reaching 48 weeks of age, the differences in indicators related to renal injury were already very evident⁶². At 60 weeks of age, SHR exhibited quite severe renal injury⁶⁵. To find a way to explore the role of BAs in the early stages of HN, we used 24-week-old SHR for our study. The SHR at this week of age had already started to show manifestations related to renal injury, but morphological manifestations were not yet evident. This is consistent with our findings that 25-week-old SHR have elevated blood pressure with impaired renal function. Next, by targeted metabolomics, we quantified the concentrations of BAs in the renal cortex of Wistar and SHR and screened for seven BAs with significantly different concentrations: DCA, CDCA, UDCA, UCA, CA, TDCA, and TCDCA. The Spearman correlation between these differential BAs and SHR blood pressure values was then analyzed, and a positive correlation was found between blood pressure values and the concentrations of differential BAs. Among them, the correlation and specificity between CA, DCA and TDCA and blood pressure values were more pronounced. In the liver, cholesterol is metabolized into primary BAs (CA and CDCA)⁶⁶. Primary BAs pass from the liver to the intestine with bile and are broken down by intestinal bacteria into secondary BAs, which are then reabsorbed by the intestine back into the liver. Elevated CA levels may lead to a decrease in aldosterone and an increase in corticosterone in the blood vessels and cause an increase in vasoconstrictor response, which ultimately induces hypertension⁶⁷. CDCA can lead to increased blood pressure in SD rats, and the possible mechanism is involved in the pathology of hypertension by inhibiting the activity of 11 β -HSD2 or 11 β -HSD1⁶⁸. Patients with CKD have been reported to exhibit altered BA homeostasis, with persistent elevation of total serum BAs in patients with different stages of CKD¹³. Among them, CA and CDCA can be important biomarkers to differentiate CKD patients from healthy patients, which was validated by the authors using different models of kidney disease⁶⁹. DCA is a form of secondary BAs, and CA is converted in the intestine by intestinal macrobacteria to DCA, which itself is a potent inhibitor of BA biosynthesis^{70–73}. Few studies have reported an association between DCA and hypertension, but DCA has been shown to exert effects on the heart, which may also cause changes in blood pressure. Elevated serum levels of BAs may be cardiotoxic, leading to cardiac dysfunction and even cardiac arrest^{74,75}. Elevated serum DCA concentrations may be related to the pathogenesis of atherosclerosis, involving the proliferation and migration of vascular smooth muscle cells⁷⁶. In another study, CKD led to an increase in DCA levels in human blood⁷⁷, and lipidomic analysis found that DCA levels were associated with coronary artery calcification volume in patients with stage 3 and 4 CKD, and that DCA plays a pathogenic role in the regulation of vascular calcification in CKD⁷⁸.

However, this study has several limitations. The number of healthy patients in the data set selected for bioinformatics analysis was small. Whilst the present study identified hub genes involved in HN, the role of these genes in the pathogenesis of HN was not verified and the specific mechanisms by which they are involved in the synthesis and breakdown of BAs were not elucidated. Consequently, subsequent studies will seek to further explore the involvement of these hub genes in HN, along with the question of which type of BAs exerts a greater impact on hypertensive kidney injury. Additionally, the relationship between different renal tissue cells and the metabolism of BAs will be investigated.

Conclusion

In conclusion, this study investigated the effect of BAs on the early stages of HN using bioinformatics combined with targeted metabolomics. Pathways such as Bile secretion are involved in the disease development of HN. Three BA-related hub genes: APOE, ALB, and SERPINA1, may be implicated in HN progression. The concentrations of multiple BAs were significantly elevated in the early stages of HN, among which, CA, DCA and TDCA were more correlated and specific for blood pressure with SHR and had a higher diagnostic value.

Data availability

In this study, publicly available datasets were analyzed, which can be found at: <https://www.ncbi.nlm.nih.gov/geo>. The data generated in the present study may be requested from the corresponding author.

Received: 6 October 2024; Accepted: 6 February 2025

Published online: 03 March 2025

References

- Griffin, K. A. Hypertensive kidney injury and the progression of chronic kidney disease. *Hypertension*. **70**(4), 687–694 (2017).
- Udani, S., Lazich, I. & Bakris, G. L. Epidemiology of hypertensive kidney disease. *Nat. Rev. Nephrol.* **7**(1), 11–21 (2011).
- Whelton, P. K. et al. 2017 ACC/AHA/AAPA/ABC/ACPM/AGS/APhA/ASH/ASPC/NMA/PCNA Guideline for the prevention, detection, evaluation, and management of high blood pressure in adults: A report of the American College of Cardiology/American Heart Association Task Force on Clinical Practice Guidelines. *J. Am. Coll. Cardiol.* **71**(19), e127–e248 (2018).
- Chen, W. C. et al. The mediating role of psychological well-being in the relationship between self-care knowledge and disease self-management in patients with hypertensive nephropathy. *Int. J. Environ. Res. Public Health*. **19**(14), 8488 (2022).
- Seccia, T. M., Caroccia, B. & Calo, L. A. Hypertensive nephropathy. Moving from classic to emerging pathogenetic mechanisms. *J. Hypertens.* **35**(2), 205–212 (2017).
- Chen, Z., Wu, H., Wang, G. & Feng, Y. Identification of potential candidate genes for hypertensive nephropathy based on gene expression profile. *BMC Nephrol.* **17**(1), 149 (2016).
- Chen, X., Cao, Y., Wang, Z., Zhang, D. & Tang, W. Bioinformatic analysis reveals novel hub genes and pathways associated with hypertensive nephropathy. *Nephrology (Carlton)*. **24**(11), 1103–1114 (2019).
- You, S. et al. Comprehensive bioinformatics analysis identifies POLR2I as a key gene in the pathogenesis of hypertensive nephropathy. *Front. Genet.* **12**, 698570 (2021).
- Di Castro, S. et al. Differential modulation of uncoupling protein 2 in kidneys of stroke-prone spontaneously hypertensive rats under high-salt/low-potassium diet. *Hypertension*. **61**(2), 534–541 (2013).
- Yang, K. et al. The protective effect of electroacupuncture on the renal cortex of SHRs: A metabolomic analysis. *Biomed. Chromatogr.* **36**(5), e5338 (2022).

11. Herman-Edelstein, M., Weinstein, T. & Levi, M. Bile acid receptors and the kidney. *Curr. Opin. Nephrol. Hypertens.* **27**(1), 56–62 (2018).
12. Wang, X. X. et al. G protein-coupled bile acid receptor TGR5 activation inhibits kidney disease in obesity and diabetes. *J. Am. Soc. Nephrol.* **27**(5), 1362–1378 (2016).
13. Levi, M. Role of bile acid-regulated nuclear receptor FXR and G protein-coupled receptor TGR5 in regulation of cardiorenal syndrome (cardiovascular disease and chronic kidney disease). *Hypertension.* **67**(6), 1080–1084 (2016).
14. Shi, H. et al. Restructuring the gut microbiota by intermittent fasting lowers blood pressure. *Circ. Res.* **128**(9), 1240–1254 (2021).
15. Ishimwe, J. A., Dola, T., Ertuglu, L. A. & Kirabo, A. Bile acids and salt-sensitive hypertension: a role of the gut-liver axis. *Am. J. Physiol. Heart Circ. Physiol.* **322**(4), H636–H646 (2022).
16. Kanehisa, M. & Goto, S. KEGG: kyoto encyclopedia of genes and genomes. *Nucleic Acids Res.* **28**(1), 27–30 (2000).
17. Kanehisa, M. Toward understanding the origin and evolution of cellular organisms. *Protein Sci.* **28**(11), 1947–1951 (2019).
18. Kanehisa, M., Furumichi, M., Sato, Y., Kawashima, M. & Ishiguro-Watanabe, M. KEGG for taxonomy-based analysis of pathways and genomes. *Nucleic Acids Res.* **51**(D1), D587–D592 (2023).
19. Shannon, P. et al. Cytoscape: a software environment for integrated models of biomolecular interaction networks. *Genome Res.* **13**(11), 2498–2504 (2003).
20. Zheng, Y. & Heagerty, P. J. Semiparametric estimation of time-dependent ROC curves for longitudinal marker data. *Biostatistics.* **5**(4), 615–632 (2004).
21. Percie du Sert, N. et al. The ARRIVE guidelines 2.0: Updated guidelines for reporting animal research. *PLoS Biol.* **18**(7), e3000410 (2020).
22. Wittig, U. & De Beuckelaer, A. Analysis and comparison of metabolic pathway databases. *Brief Bioinform.* **2**(2), 126–142 (2001).
23. Denny, P. et al. Exploring autophagy with Gene Ontology. *Autophagy.* **14**(3), 419–436 (2018).
24. Yang, K., Zhang, P., Lv, T., Wu, J. & Liu, Q. Acupuncture at Taichong and Zusanli points exerts hypotensive effect in spontaneously hypertensive rats by metabolomic analysis. *J. Chromatogr B Analyt. Technol. Biomed. Life Sci.* **1207**, 123352 (2022).
25. Li, X. et al. Combination of *Oxalobacter formigenes* and *Veillonella parvula* in gastrointestinal microbiota related to bile-acid metabolism as a biomarker for hypertensive nephropathy. *Int. J. Hypertens.* **2022**, 5999530 (2022).
26. Meyrier, A. Nephrosclerosis: update on a centenarian. *Nephrol. Dial. Transplant.* **30**(11), 1833–1841 (2015).
27. Hill, G. S. Hypertensive nephrosclerosis. *Curr. Opin. Nephrol. Hypertens.* **17**(3), 266–270 (2008).
28. Schulz, A. & Kreutz, R. Mapping genetic determinants of kidney damage in rat models. *Hypertens. Res.* **35**(7), 675–694 (2012).
29. Kirilenko, B. M., Hagey, L. R., Barnes, S., Falany, C. N. & Hiller, M. Evolutionary analysis of bile acid-conjugating enzymes reveals a complex duplication and reciprocal loss history. *Genome Biol. Evol.* **11**(11), 3256–3268 (2019).
30. Yu, A. et al. Altered O-glycomes of renal brush-border membrane in model rats with chronic kidney diseases. *Biomolecules.* **11**(11), 1560 (2021).
31. Sabino-Silva, R. et al. SGLT1 protein expression in plasma membrane of acinar cells correlates with the sympathetic outflow to salivary glands in diabetic and hypertensive rats. *Am. J. Physiol. Endocrinol. Metab.* **299**(6), E1028–E1037 (2010).
32. Li, C. et al. Long noncoding RNA p21 enhances autophagy to alleviate endothelial progenitor cells damage and promote endothelial repair in hypertension through SESN2/AMPK/TSC2 pathway. *Pharmacol. Res.* **173**, 105920 (2021).
33. Cheng, L. et al. Clinically relevant high levels of human C-reactive protein induces endothelial dysfunction and hypertension by inhibiting the AMPK-eNOS axis. *Clin. Sci. (Lond).* **134**(13), 1805–1819 (2020).
34. Zhang, J. et al. The E3 ubiquitin ligase TRIM31 plays a critical role in hypertensive nephropathy by promoting proteasomal degradation of MAP3K7 in the TGF-beta1 signaling pathway. *Cell Death Differ.* **29**(3), 556–567 (2022).
35. Shi, H. H. et al. EPA-enriched phospholipids alleviate renal interstitial fibrosis in spontaneously hypertensive rats by regulating TGF-beta signaling pathways. *Mar. Drugs.* **20**(2), 152 (2022).
36. Wiese, O., Zemlin, A. E. & Pillay, T. S. Molecules in pathogenesis: angiotensin converting enzyme 2 (ACE2). *J. Clin. Pathol.* **74**(5), 285–290 (2021).
37. Wang, Z. et al. Naringenin ameliorates renovascular hypertensive renal damage by normalizing the balance of renin-angiotensin system components in rats. *Int. J. Med. Sci.* **16**(5), 644–653 (2019).
38. Attman, P. O., Alaupovic, P. & Samuelsson, O. Lipoprotein abnormalities as a risk factor for progressive nondiabetic renal disease. *Kidney Int. Suppl.* **71**, S14–S17 (1999).
39. Cases, A. & Coll, E. Dyslipidemia and the progression of renal disease in chronic renal failure patients. *Kidney Int. Suppl.* **99**, S87–93 (2005).
40. Dalrymple, L. S. & Kaysen, G. A. The effect of lipoproteins on the development and progression of renal disease. *Am. J. Nephrol.* **28**(5), 723–731 (2008).
41. Keane, W. F. The role of lipids in renal disease: future challenges. *Kidney Int. Suppl.* **75**, S27–31 (2000).
42. Kim, H. J., Moradi, H., Yuan, J., Norris, K. & Vaziri, N. D. Renal mass reduction results in accumulation of lipids and dysregulation of lipid regulatory proteins in the remnant kidney. *Am. J. Physiol. Renal Physiol.* **296**(6), F1297–F1306 (2009).
43. Liberopoulos, E., Siamopoulos, K. & Elisaf, M. Apolipoprotein E and renal disease. *Am. J. Kidney Dis.* **43**(2), 223–233 (2004).
44. Nogueira, B. V., Peotta, V. A., Meyrelles, S. S. & Vasquez, E. C. Evaluation of aortic remodeling in apolipoprotein E-deficient mice and renovascular hypertensive mice. *Arch. Med. Res.* **38**(8), 816–821 (2007).
45. Vaziri, N. D. et al. Amelioration of nephropathy with apoA-1 mimetic peptide in apoE-deficient mice. *Nephrol. Dial. Transplant.* **25**(11), 3525–3534 (2010).
46. Shi, J. et al. Association between ApoE polymorphism and hypertension: A meta-analysis of 28 studies including 5898 cases and 7518 controls. *Gene.* **675**, 197–207 (2018).
47. Wang, C., Yan, W., Wang, H., Zhu, J. & Chen, H. APOE polymorphism is associated with blood lipid and serum uric acid metabolism in hypertension or coronary heart disease in a Chinese population. *Pharmacogenomics.* **20**(14), 1021–1031 (2019).
48. Endres, B. T. et al. Intravital imaging of the kidney in a rat model of salt-sensitive hypertension. *Am. J. Physiol. Renal Physiol.* **313**(2), F163–F173 (2017).
49. Bruno, R. M. et al. Predictive role of renal resistive index for clinical outcome after revascularization in hypertensive patients with atherosclerotic renal artery stenosis: a monocentric observational study. *Cardiovasc. Ultrasound.* **12**, 9 (2014).
50. Yoshida, M. et al. Analysis of genes causing hypertension and stroke in spontaneously hypertensive rats: gene expression profiles in the brain. *Int. J. Mol. Med.* **33**(4), 887–896 (2014).
51. Baraldo, S. et al. Alpha-1 antitrypsin deficiency today: new insights in the immunological pathways. *Respiration.* **91**(5), 380–385 (2016).
52. Bristow, C. L. et al. A feedback regulatory pathway between LDL and alpha-1 proteinase inhibitor in chronic inflammation and infection. *Discov. Med.* **16**(89), 201–218 (2013).
53. Gordon, S. M. et al. Rosuvastatin alters the proteome of high density lipoproteins: generation of alpha-1-antitrypsin enriched particles with anti-inflammatory properties. *Mol. Cell Proteomics.* **14**(12), 3247–3257 (2015).
54. Kotani, K., Yamada, T. & Taniguchi, N. The association between adiponectin, HDL-cholesterol and alpha1-antitrypsin-LDL in female subjects without metabolic syndrome. *Lipids Health Dis.* **9**, 147 (2010).
55. Lisowska-Myjak, B., Pachecka, J., Witak, P. & Radowski, S. Comparison of urinary excretion of albumin and alpha-1-antitrypsin in patients with arterial hypertension. *Scand. J. Clin. Lab. Invest.* **59**(2), 93–97 (1999).

56. Starodubtseva, N. et al. SERPINA1 peptides in urine as a potential marker of preeclampsia severity. *Int. J. Mol. Sci.* **21**(3), 914 (2020).
57. Curjuric, I. et al. Alpha-1 antitrypsin deficiency: From the lung to the heart?. *Atherosclerosis*. **270**, 166–172 (2018).
58. Choi, Y. W. et al. Potential urine proteomics biomarkers for primary nephrotic syndrome. *Clin. Proteomics*. **14**, 18 (2017).
59. Ferkingstad, E. et al. Genome-wide association meta-analysis yields 20 loci associated with gallstone disease. *Nat. Commun.* **9**(1), 5101 (2018).
60. Wang, S., Sheng, F., Zou, L., Xiao, J. & Li, P. Hyperoside attenuates non-alcoholic fatty liver disease in rats via cholesterol metabolism and bile acid metabolism. *J. Adv. Res.* **34**, 109–122 (2021).
61. Hultstrom, M. Development of structural kidney damage in spontaneously hypertensive rats. *J. Hypertens.* **30**(6), 1087–1091 (2012).
62. Zhang, Z., Wang, F. Z., Li, Z. X. & Song, X. R. Telmisartan attenuates the growth of epithelium-like cells and glomerular injury in spontaneously hypertensive rats. *Curr. Med. Sci.* **41**(3), 498–504 (2021).
63. Bakoush, O. et al. Increased glomerular albumin permeability in old spontaneously hypertensive rats. *Nephrol. Dial. Transplant.* **19**(7), 1724–1731 (2004).
64. Feld, L. G., Van Liew, J. B., Galaske, R. G. & Boylan, J. W. Selectivity of renal injury and proteinuria in the spontaneously hypertensive rat. *Kidney Int.* **12**(5), 332–343 (1977).
65. Hultstrom, M., Leh, S., Skogstrand, T. & Iversen, B. M. Upregulation of tissue inhibitor of metalloproteases-1 (TIMP-1) and procollagen-N-peptidase in hypertension-induced renal damage. *Nephrol. Dial. Transplant.* **23**(3), 896–903 (2008).
66. Chiang, J. Y. Bile acid metabolism and signaling. *Compr. Physiol.* **3**(3), 1191–1212 (2013).
67. Wu, P. et al. Effects of cholic acid on blood pressure and production of vascular aldosterone and corticosterone. *Steroids*. **64**(4), 291–295 (1999).
68. Morris, D. J. & Souness, G. W. Endogenous 11 beta-hydroxysteroid dehydrogenase inhibitors and their role in glucocorticoid Na⁺ retention and hypertension. *Endocr. Res.* **22**(4), 793–801 (1996).
69. Chen, H. et al. Metabolomics insights into activated redox signaling and lipid metabolism dysfunction in chronic kidney disease progression. *Redox Biol.* **10**, 168–178 (2016).
70. Heuman, D. M., Vlahcevic, Z. R., Bailey, M. L. & Hylemon, P. B. Regulation of bile acid synthesis II Effect of bile acid feeding on enzymes regulating hepatic cholesterol and bile acid synthesis in the rat. *Hepatology*. **8**(4), 892–897 (1988).
71. Xu, G. et al. Glycocholic acid and glycodeoxycholic acid but not glycoursocholic acid inhibit bile acid synthesis in the rabbit. *Gastroenterology*. **102**(5), 1717–1723 (1992).
72. LaRusso, N. F., Szczepanik, P. A. & Hofmann, A. F. Effect of deoxycholic acid ingestion on bile acid metabolism and biliary lipid secretion in normal subjects. *Gastroenterology*. **72**(1), 132–140 (1977).
73. Stange, E. F., Scheibner, J. & Ditschuneit, H. Role of primary and secondary bile acids as feedback inhibitors of bile acid synthesis in the rat in vivo. *J. Clin. Invest.* **84**(1), 173–180 (1989).
74. Desai, M. S. et al. Bile acid excess induces cardiomyopathy and metabolic dysfunctions in the heart. *Hepatology*. **65**(1), 189–201 (2017).
75. Vasavan, T. et al. Heart and bile acids—Clinical consequences of altered bile acid metabolism. *Biochim. Biophys. Acta Mol. Basis Dis.* **1864**(4), 1345–1355 (2018).
76. Shimizu, H. et al. Deoxycholic acid is involved in the proliferation and migration of vascular smooth muscle cells. *J. Nutr. Sci. Vitaminol. (Tokyo)*. **60**(6), 450–454 (2014).
77. Miyazaki-Anzai, S. et al. Free deoxycholic acid exacerbates vascular calcification in CKD through ER stress-mediated ATF4 activation. *Kidney360*. **2**(5), 857–868 (2021).
78. Jovanovich, A. et al. Deoxycholic acid, a metabolite of circulating bile acids, and coronary artery vascular calcification in CKD. *Am. J. Kidney Dis.* **71**(1), 27–34 (2018).

Acknowledgements

The Animal Care and Utilization Committee of Beijing University of Traditional Chinese Medicine approved this study (BUCM-4-2021-041001-2093). This research report was conducted in accordance with the relevant guidelines and regulations and also all methods are reported in accordance with ARRIVE guidelines.

Author contributions

KZY, FCW: Methodology, Writing – original draft, Writing – review & editing. GY: Software, Data curation, Formal analysis, Writing – review & editing. XFD, LZ: Software, Conceptualization, Writing – review & editing. JPL, YY: Validation, Writing – review & editing. JHL, QGL: Writing – original draft, Validation. PNZ, JQF: Writing – original draft, Writing – review & editing.

Funding

This work was supported by the National Natural Science Foundation of China (No. 82074553), Zhejiang Provincial Natural Science Foundation of China (No. LQN25H270003), Zhejiang Province Traditional Chinese Medicine Science and Technology Project (No. 2025ZR150).

Declarations

Competing interests

The authors declare no competing interests.

Additional information

Supplementary Information The online version contains supplementary material available at <https://doi.org/10.1038/s41598-025-89601-0>.

Correspondence and requests for materials should be addressed to K.Y. or F.W.

Reprints and permissions information is available at www.nature.com/reprints.

Publisher's note Springer Nature remains neutral with regard to jurisdictional claims in published maps and institutional affiliations.

Open Access This article is licensed under a Creative Commons Attribution-NonCommercial-NoDerivatives 4.0 International License, which permits any non-commercial use, sharing, distribution and reproduction in any medium or format, as long as you give appropriate credit to the original author(s) and the source, provide a link to the Creative Commons licence, and indicate if you modified the licensed material. You do not have permission under this licence to share adapted material derived from this article or parts of it. The images or other third party material in this article are included in the article's Creative Commons licence, unless indicated otherwise in a credit line to the material. If material is not included in the article's Creative Commons licence and your intended use is not permitted by statutory regulation or exceeds the permitted use, you will need to obtain permission directly from the copyright holder. To view a copy of this licence, visit <http://creativecommons.org/licenses/by-nc-nd/4.0/>.

© The Author(s) 2025